A Three-Function Numerical Model for the Prediction of Vulcanization-Reversion of Rubber During Sulfur Curing

G. Milani,[1] F. Milani[2]

[1]*Department of Structural Engineering (DIS), Politecnico di Milano, Piazza Leonardo da Vinci 32, 20133 Milano, Italy*
[2]*Chem.CO Consultant, Via J. F. Kennedy 2, 45030 Occhiobello, Rovigo, Italy*

Received 31 October 2009; accepted 13 April 2010
DOI 10.1002/app.32670
Published online 27 July 2010 in Wiley Online Library (wileyonlinelibrary.com).

ABSTRACT: The cross-linking mechanisms of sulfur vulcanization are not analytically known and, therefore, reticulation kinetics has to be deduced macroscopically from standardized tests. One of the most popular laboratory test to characterize curing and reversion is the oscillating disk rheometer ODR, which gives a quantitative assessment of scorch, cure rate, and state of cure. In this article, a numerical two-step approach, which is based on the utilization of experimental ODR data and aimed at predicting the degree of vulcanization of thick rubber items cured with accelerated sulfur, is presented. In step one, a composite numerical three-function curve is used to fit experimental rheometer data, able to describe the increases of the viscosity at successive curing times and at different controlled temperatures, requiring only few points of the experimental cure curve to predict the global behavior. Both the case of indefinite increase of the torque and reversion can be reproduced with the model. In step two, considering the same rubber compound of step one, numerical cure curves at different temperatures are collected in a database and successively implemented in a Finite Element software, which is specifically developed to perform thermal analyzes on complex 2D/3D geometries. As an example, an extruded thick EPDM section is considered and meshed through eight-noded isoparametric plane elements. Several FEM simulations are repeated by changing exposition time t_c and external curing temperature T_n, to evaluate for each (t_c,T_n) couple the corresponding mechanical properties of the item at the end of the thermal treatment. A recently presented bisectional approach, alternating tangent (AT), is used to drastically reduce the computational efforts required to converge to the optimal solution associated with the maximum value of an output property, tensile strength. J Appl Polym Sci 119: 419–437, 2011

Key words: sulfur vulcanization; reversion; rheometer curve fitting; Fourier's law of heat conduction; finite element method

INTRODUCTION

Chemical reactions associated with sulfur vulcanization are complex and involve only a few atoms in each polymer molecule; therefore, to propose a quantitative macroscopic model to predict vulcanization in terms of the physical properties of the rubber is not an easy task.

Sulfur is used in combination with one or more accelerators (e.g. sulfenamides, thiazoles, thiuram sulfides, etc.) and an activator system, as for instance soluble zinc (which increases drastically the efficiency of cross-linking formation[1]) and fatty acid.[2] In this context, many reagents are nowadays at disposal associated with sulfur vulcanization of polydienes.[3,4]

However, despite the spreading of such kind of curing technique, the chemistry of vulcanization with sulfur has not been well understood, since its discovery by Goodyear in 1839[5–7], because of the complexity of the reactions induced by sulfur during cross-linking[6,7], Figure 1. Contrarily to peroxidic curing, no reaction kinetics formulas are available in the technical literature. In this field, among the others, historical contributions by Ding and Leonov[8] and Ding et al.[9] are worth noting. They are numerical approaches in which the models are enforced to resemble to peroxide laws.

Another important aspect is the so-called reversion of the compound. Reversion occurs quite frequently in practice and, from a macroscopic point of view, it consists in a remarkable decrease or rubber vulcanized properties at the end of the curing process. Chen et al.[10] have shown that this phenomenon seems to appear when two reactions are competing during vulcanization. Reversion is often associated with high temperature curing. For instance, Loo[11] demonstrated that, as the cure temperature rises, the cross-link density drops, thus increasing the degree of reversion. Morrison and Porter[12] confirmed that the observed reduction in vulcanizate properties is

Correspondence to: G. Milani (gabriele.milani@polimi.it).

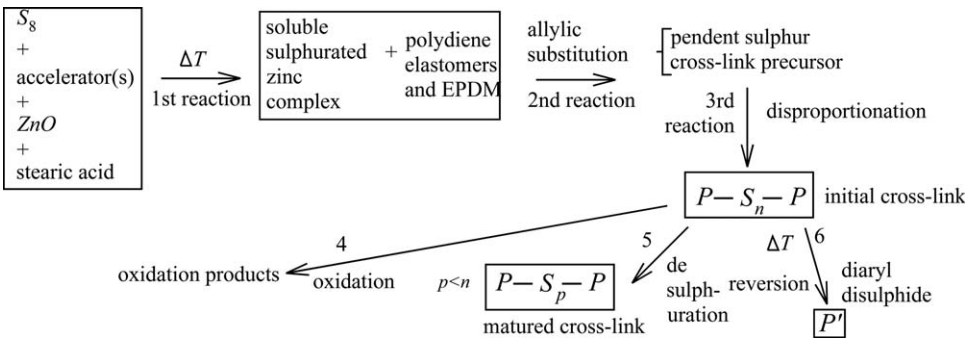

Figure 1 Products and schematic reaction mechanisms of accelerated sulfur vulcanization of polydiene and EPDM elastomers.

caused by two reactions proceeding in parallel, that is, desulfuration and decomposition, see Figure 1. Despite that all these phenomena have been observed and widely interpreted from a chemical point, they remain, at present, under-investigated numerically.

In this framework, experimentation may represent a good starting point to collect macroscopic information on the degree of cross-linking. One of the most diffused laboratory tests to characterize curing and reversion is the so-called oscillating disc rheometer, a device with biconical shape oscillating in a rubber specimen at constant temperature (ASTMD 2084-81).[13] During the test, the resistance to oscillation (torque) is measured in continuous and recorded as a function of the time in the so-called cure curve (or rheometer curve). The cure curve gives an indirect macroscopic information on rubber reticulation kinetics at fixed temperature. The torque varies during the test, with a typical decrease in the initial stage, followed by a sudden increase at $\sim 1/3$ of the time needed to complete the test (scorch time). In several cases, torque decreases near the end of the experimentation, exhibiting reversion. A single compound has its own characteristic cure curve at fixed temperature, which characterizes macroscopically the reticulation of the compound. A change in both accelerators molar ratios and temperature room changes the cure curve.

The aim of this work is to propose a combined experimental and numerical model able to predict macroscopically the effect of accelerated sulfur curing, with particular emphasis on the numerical reproduction of reversion.[1,14,15]

The approach is a two-step procedure. In the first step, for a given rubber compound, rheometer curves have to be experimentally evaluated at different vulcanization temperatures, ranging from low to high. Unfortunately, cure curves on the same compound at different temperatures are not easily available in the literature and, in any case, experimental data are not sufficiently smooth to be implemented in a numerical model devoted to the prediction of the vulcanization level of a real rubber item industrially cured with sulfur. For this reason, in the first step, a three function composite curve is proposed to fit as close as possible experimental data available.

The second step relies in implementing the curves collected in the database in a thermal analysis conducted through Finite Elements. Thermal analyzes are performed on real thick items to vulcanize industrially. Such analyzes are nonstandard and required the noncommercial implementation of a software able to consider the dependence of mechanical and thermal parameters of the compound with respect to temperature and cure curves. The software developed allows to obtain, element by element, temperature profiles at increasing curing times and the increase of output mechanical properties (tensile strength, tear resistance, elongation) as a function of curing time, passing through the numerical database collected in step 1. As a matter of fact, each point of the item undergoes different temperatures, with considerable differences passing from the skin to the core. The corresponding cross-linking density level for each point of the item is numerically evaluated[1,16] at fixed exposition time throughout the database collected in the first step (rheometer curves), allowing an estimation point by point of any output mechanical property.

To assess the capabilities of the two step approach proposed, in this article, an example of engineering interest is analyzed in detail, consisting of a rubber thick item with rectangular shape (dimensions 35× 40 mm) and a central circularly shaped hole of diameter equal to 15 mm. The compound used to realize the cylinder is an EPDM rubber with a medium amount of propylene content (about 40% in weight) and 4.5% in weight on ENB, vulcanized through accelerated sulfur, as described in detail next.

A recently presented bisectional procedure (alternating tangent approach AT)[17,18] is implemented to

determine, with a very limited computational effort, optimal input parameters (curing external temperature T_n and rubber exposition time t_c) for the example at hand. Output mechanical property (objective function) to optimize is represented by the average tensile strength of the item.

It is authors' opinion that the reversion problem[14,15] during accelerated sulfur curing is a very difficult task to reproduce numerically. Indeed, this reaction depends on several concurring factors, as for instance the elastomer typology, the concentration of active double bonds, the quality of all the components (including filler), and their reciprocal concentrations. In this framework, this work is aimed at putting the bases for a substantial review of the interpretation of sulfur vulcanization, aimed at optimizing output mechanical properties of real thick items. From an industrial point of view, the numerical approach proposed could lead to optimize (also in economical terms) (i) vulcanization time, (ii) energy utilization, (iii) temperature of vulcanization, and (iv) accelerators quantities. The approach is general and can be used in presence of any rubber compound, provided that suitable experimental data are at disposal to characterize cross-linking reactions at different temperatures. A full experimental campaign is planned by the authors comprising both (a) the collection of a detailed database of cure curves at different temperatures and varying compound typology and (b) the vulcanization of full scale industrial items varying both curing time and vulcanization external temperatures.

THE OSCILLATING DISK CURE METER

At present, some standardized experimental tests to evaluate macroscopically the vulcanization characteristics of vulcanizable rubber compounds are at disposal, as for instance the oscillating disk cure meter (ODR-ASTM D 2084).[13]

The ODR is a traditional approach, which now can be substituted with other technologies, as for instance RPA 2000, rotorless curometers introduced in 1980s, etc. Despite this important remark, ODR still remains used by many authors to characterize the cure level of elastomers, see for example.[19–21]

Here, it should be stressed that experimental data considered hereafter (cure curve vs final tensile strength) are obtained using an ODR, and therefore the reference to the oscillating disk rheometer still remains meaningful in this context. Nonetheless, the advantages related to the used of, for example, RPA 2000 instead of ODR must be emphasized, having in mind that the numerical approach proposed is strictly methodological, as it is tailored to fit macroscopic experimental data (e.g. a general cure curve) provided by any experimental apparatus (ODR, DSC, MDR). To have a better insight into pros and cons of ODR, DSC, and MDR, comparing also output information provided, the reader is referred to.[22,23]

As a matter of fact, one of the well known advantages of MDR is that the elastic torque response (S′) is in-phase with the applied strain whereas the viscous torque response (S″) is 90° out-of-phase with the applied strain. This implies that ODR cannot measure S″ with precision because of friction associated with the rotor. Therefore, the shape of a typical S″ cure curve from a rotorless curemeter is very different from the conventional S′ cure curve in either an oscillating disk curemeter or a rotorless curemeter.

Nonetheless, the target of the article is not only to focus on the typology of technology used but also on the output data provided experimentally. In any case, these data represent the only very preliminary step to be used within a thermal analysis performed using FEM.

In the ODR, the resistance to oscillation (torque) is measured and recorded as a function of the time, as in Figure 2. In practice, three different cases can occur, as shown in Figure 2: (a) the curve reaches a maximum asymptotically, (b) the curve reaches a maximum and then decreases (reversion), and (c) the curve increases monotonically after the scorching time t_2. The second case is encountered very frequently in practice, because reversion is a distinguishing characteristic of sulfur curing (Fig. 1), especially at high temperatures.

In Figure 2, we define the following characteristic times t_2 scorch, t_{90} and t_{100} times. Scorch time t_2 is defined as the time to incipient cure. A torque equal to M_2 corresponds to t_2. From a mathematical point of view, it may represent, for instance, the point at which second derivative of the rheometer curve is equal to zero. The t_{90} is approximately the time at which 90% of cross-linking is occurred, whereas t_{100} is the time at which the experimentation ends (corresponding torque value: M_{HF}). Finally, it is interesting to notice that the cure curve exhibits also a minimum point (coordinates: t_m–M_m), reached soon during the experimentation in the rheometer.

Experimental data fitting through a composite three function curve

The numerical algorithm proposed is based on the experimental use of rheometers following the ASTM D 2084 method[13] at different temperatures to collect a suitable database of experimental data regarding cure curves (e.g. t_m, t_2, t_{90}, M_m, M_2, M_{HF}) at increasing temperatures and their successive interpolation by means of a simple mathematical formulation.

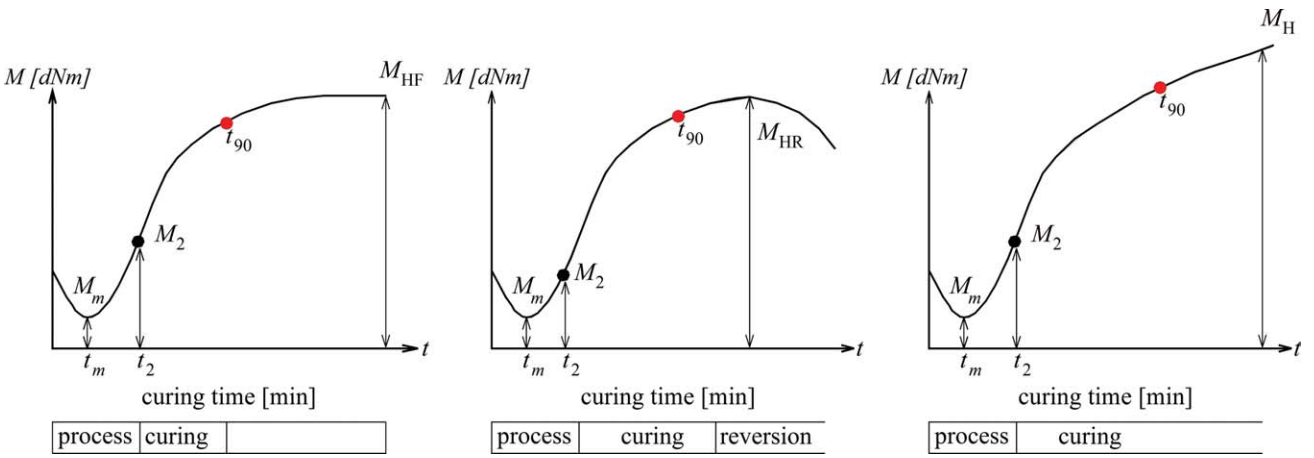

Figure 2 Typical experimental behavior of a rubber compound during rheometer test. [Color figure can be viewed in the online issue, which is available at wileyonlinelibrary.com.]

At present, the knowledge regarding the chemistry of accelerated sulfur vulcanization seems a bit fragmented; some useful experimental data are available from Poh et al.,[24–29] who observed a marked relation among scorch time, amount of activators used and rheometer temperatures.

However, data reported in the literature are insufficient to fully calibrate the numerical model here proposed. In fact, to predict the vulcanization rate during an industrial process of production of thick items, it is necessary to have at disposal from laboratory experimentation, several "characteristic points" of the rheometer curve for the same rubber recipe at different controlled curing temperature inside the oscillating rheometer.

In particular, it is necessary to know (at least) the minimum point of the cure curve, scorch time (with its torque value), t_{90} and torque value after full vulcanization. These values allow to post-process experimental results and approximate the cure curve with simple mathematical functions (e.g. parabolas and hyperbole, as shown in the previous subsection).

The mathematical approximation used to reproduce numerically a typical cure curve is represented in Figure 3, and it relies in approximating experimental data by means of a three-function composite first derivative continuous curve represented by two parabolas and a rectangular hyperbola with asymptotes rotated of a predetermined θ angle with respect to the horizontal axis.

Only four points of the experimental cure curve are needed, for instance the minimum point (square), the scorch point (triangle), and other 2 points for the rotated hyperbola. If available from experimentation, they could be for instance points with abscissa equal to t_{90} and t_{100} (maximum point). Nevertheless, it is worth noting that it is not strictly necessary to consider t_{90} and and t_{100} to mathematically calibrate hyperbola, but any point may be chosen depending on the fitting performance of the three functions curve. First parabola holds in the time range between zero and t_2, second parabola between t_2 and t_{90}, and hyperbola after t_{90}. Obviously, this concept may be repeated for all the other points considered. However, the aim of the approach proposed is to allow to conduct fast experimental campaigns where only few points of the cure curves are collected. Furthermore, a physical interpretation is at the base of the choice adopted. The first parabola corresponds to a viscous status of the compound before the vulcanization is started, the second curve represents the fast curing process (e.g. allylic substitution, cross-linking precursion formation, cross-linking reaction), whereas the last curve is the combination of the second step with oxidation, desulfuration, and reversion.

More in detail, equations of the composite mathematical cure curve are the following:

$$\begin{gathered} M(t) = a_1 t^2 + b_1 t + c_1 \\ t(M) = a_2 M^2 + b_2 M + c_2 \\ \left(M + \frac{t}{\tan\vartheta} + a_3\right)(M - \tan\vartheta t + b_3) = c_3 \end{gathered} \tag{1}$$

As a first substep, constants a_1, b_1, and c_1 are determined by imposing that the first parabola passes through the scorching point and has a minimum located at the experimental minimum of the cure curve (two algebraic conditions).

It is worth noting that eq. (1) is just empirical and coefficients do not have a precise physical meaning. A correlation between cure curve fitting and reticulation kinetics (following, for instance, what proposed by Ding and Leonov)[8] is avoided to present an easy to use empirical numerical model, able to give only macroscopic information on vulcanized items.

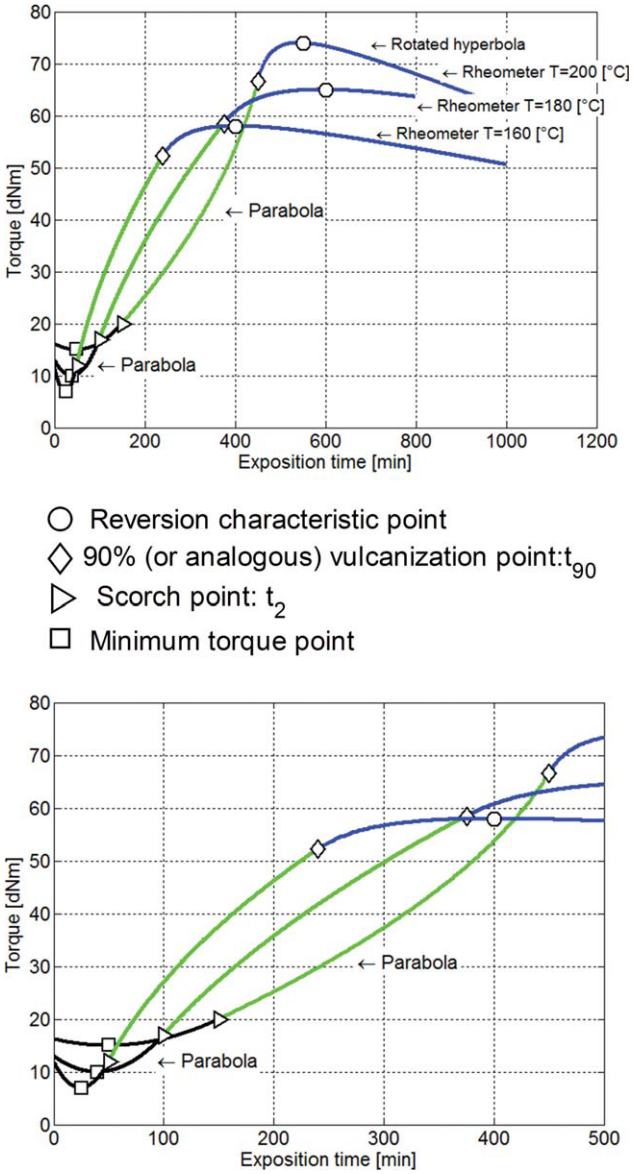

Figure 3 Numerical three function composite curve to simulate rheometer test and reversion. [Color figure can be viewed in the online issue, which is available at wileyonlinelibrary.com.]

Afterward, the second parabola (with horizontal axis) is determined imposing the passage through the scorching point and assuming that first and second parabola have the same first derivative at the scorching point. This latter requirement, through the well-known theorem of first derivative of the inverse function, reduces to the following condition:

$$2a_1t_2 + b_1 = \frac{1}{2a_2M_2 + b_2} \tag{2}$$

Finally, hyperbola is analytically determined imposing (i) the passage through, for example, t_{90}, (ii) the common tangent in t_{90} with the second parabola, and (iii) the passage condition through a further point, for instance (t_{100};M_{HF}). It is worth underlining that the asymptotes rotation angle θ has to be a priori chosen with a posteriori evaluation of the fitting performance of reversion phenomenon. Finally, it is worth noting that the model is sufficiently general to reproduce also horizontal plateaus (ideal behavior without reversion) and indefinitely increasing cure curves.

To evaluate the fitting capabilities of the model proposed, numerical curves must be compared with full experimental data available in the literature.

In this context, four experimental cure curves collected from[21] are hereafter considered. Experimental cure curves correspond to four different compounds in which zinc salts at molar equivalency 5.0 phr zinc oxide, 12.8 phr ZDA, 14.5 phr ZDMA, and 10.4 phr ZMMA are used as activators. Rubber used is Goodyear Natsyn 2200 ® and the reader is referred to[21] for a detailed description of the compound.

ZDA indicates a zinc diacrylate produced by Sartomer (Sartomer SR705, Sartomer Inc. Exton, Pennsylvania), ZDMA is a zinc di-metacrylate (Sartomer SR708), whereas ZMMA is a zinc mono-metacrylathe (Sartomer SR709).

Scorching time and values of torque to use in the numerical approximation of the experimental data are collected from.[21] Experimental cure curves are obtained at 160° following ASTMD 2084-81,[13] using an arc deflection of 3°. In Figure 4, a full comparison between experimental data provided using the four activators analyzed and the numerical approximation here proposed is represented. As it is possible to notice, in all the cases analyzed a very good agreement is found, with an almost perfect fitting of reversion, especially in the first, second, and last example.

As second example to validate the numerical model in presence of a marked reversion, we analyze again a Goodyear Natsyn 2200 ® compound vulcanized exclusively with ZDMA (except for one case, where ZnO has been used) at decreasing concentrations of ZDMA accelerator, Table I. Full experimental cure curves are available from,[21] some of them exhibiting reversion. In particular, it is interesting to notice that a reduction of the accelerator concentration in the compound, results in an increase of reversion, which becomes quite predominant at small concentrations of the accelerator. This is a common issue of sulfur vulcanization and is well-documented in the literature.[14,15] A full comparison between experimental cure curves and present numerical predictions is provided in Figure 5. Very good agreement is found also in presence of marked reversion. In the last case (ZDMA 1.81 phr), an high reversion is present (around 30% at the end of the curing process).

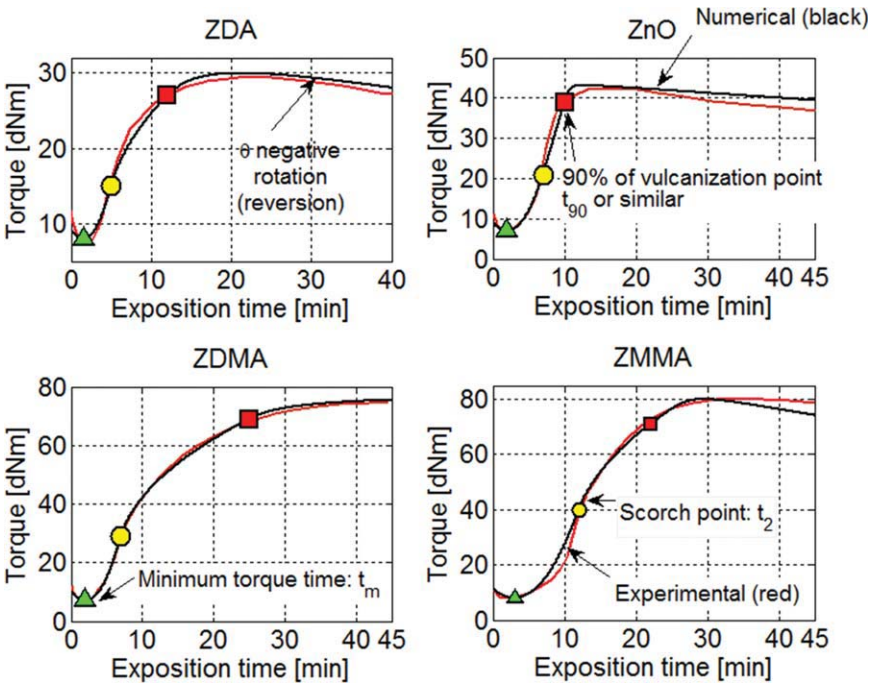

Figure 4 Comparison between experimental data [21] and the numerical three function curve proposed. [Color figure can be viewed in the online issue, which is available at wileyonlinelibrary.com.]

From simulations results, it is particularly evident that the numerical model proposed may furnish a quantitative information of reversion at a fixed compound, suitable to establish the most indicated production parameters to use. This could allow to reduced economical losses of real production plants, which are usually designed following simple rule of thumbs.

Nevertheless, it is worth underlining that, to predict correctly input parameters to optimize the vulcanization of thick items, it is necessary to have at disposal cure curves of the same compound at different temperatures. Such curves (or only meaningful points) are collected in a database and fitted numerically with the procedure proposed.

In this framework, some experimental data regarding rubber compounds exhibiting reversion have been collected from existing literature. In particular, an EPDM compound (Dutral 4334 by Polimeri Europa) with the following percentages in weight have been tested in the oscillating disk at 160 and 200°C: propylene 27%, paraffinic oil 30%, and ENB 4.5%. The experimental formulation is the following: 140 phr of polymer, 115 phr of filler carbon black (N330), 3 phr of zinc oxide, 2.5 phr of stearic acid, 1.2 phr of 2-mercaptobenzothiazole, 0.8 phr of tetramethylthiuram disulfide, 1.8 of zinc dibutyldithiocarbamide, and 2 phr of sulfur. The Mooney viscosity of the compound at 100°C was equal to 90. The characteristic times (t_2, t_{90}, etc.) along with the corresponding torque at the different temperatures inspected are summarized in Table II.

From data collected in Table II, the mathematical approximation of the cure curves at different temperatures reported in Figure 6 have been obtained with the model proposed. Such curves will be used in the following section to predict the optimal vulcanization of a thick item industrially produced.

Cured rubber mechanical properties

To evaluate numerically the degree of vulcanization of a given rubber item, it is necessary to link degree of vulcanization with output mechanical properties. There are many important parameters that producers are interested to maximize at the end of the vulcanization process as for instance tear resistance, tensile strength, tension set, etc.[30,31] Unfortunately, in almost the totality of the cases, such parameters cannot be maximized at the same time. In this

TABLE I
Composition of the Compound Analyzed in Figure 5 (cure temperature 160°C)

Ingredient	phr
Natsyn 2200 Goodyear [Polyisoprene (cis-1.4)]	100
N330 Carbon Black Cabot Vulcan 1345	50
Processing oil [Sunoco Sunpar 2280]	10
ZnO	variable
Stearic Acid	2
ZDMA (Sartomer SR708) [Zinc dimethacrylate]	variable
Atioxidant-Uniroyal Chemical Naugard Q (TMQ)	1
TBBS [N-t-butylbenzothiazole-2-sulfenamide]	0.7
Sulfur	2.5

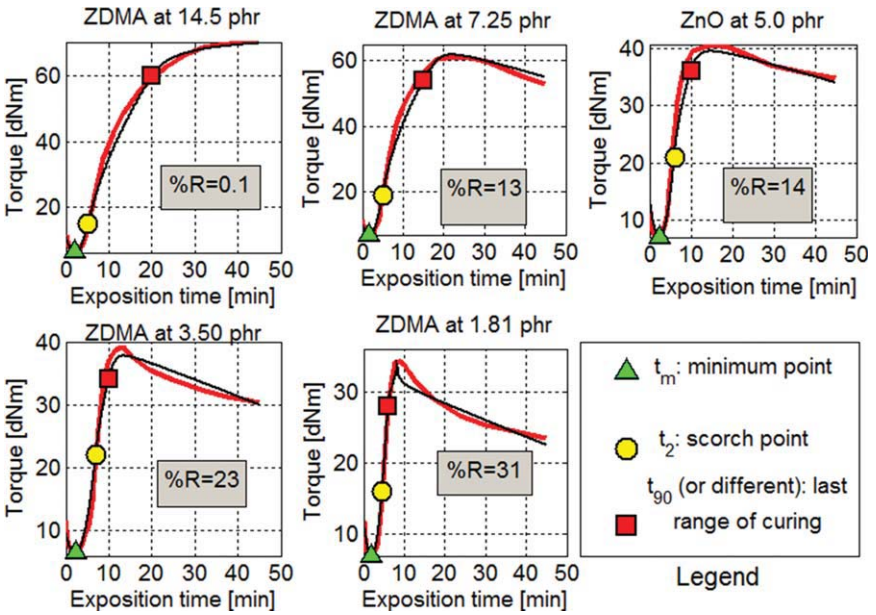

Figure 5 Comparison between experimental data[21] and the numerical three functions curve proposed. The formulation of the compound analyzed is reported in Table I; four different amounts of ZDMA –zinc dimethacrylate Sartomer SR708- (14.5, 7.25, 3.50, and 1.81 phr) and one of ZnO (5.0 phr) have been compared. The reversion % (%R) has been indicated in the subfigures. [Color figure can be viewed in the online issue, which is available at wileyonlinelibrary.com.]

article, we will focus, for the sake of simplicity, only on a single output parameter (tensile strength).

As experimental evidences show, there is a precise relationship between torque values obtained in the cure curve and output mechanical properties of a real vulcanized item.[21]

In Figure 7, several experimental data[21] collected in the literature concerning torque values M and tensile strength are represented, along with a possible numerical experimental data fitting.

As data are collected from different experimentations and different compounds (Dutral 4334 and Natsyn 2200+Sartomer), different curves are needed to fit experimental data. The numerical relation between torque and tensile strength reported in Figure 7 will be used in the following section to perform some simulations on real thick rubber items. When dealing with Dutral 4334 compound, experimental values of output tensile strength are also available in Table III.

An interesting aspect of the experimental relation existing between torque and tensile strength is that such relation is not necessarily monotonic, that is, tensile strength may decrease increasing torque resistance. Because of the lack of a sufficient amount of experimental data available in the literature concerning this issue, we will repeat numerical simulations assuming both a monotonic and a nonmonotonic behavior for the compound, always in presence of a significant level of reversion.

Another important aspect to underline is that, obviously, the representation of Figure 7 is able to give correct information on output parameters only at constant temperatures (note that $T \neq T_n$, being T rubber temperature), that is, results cannot be applied directly to a rubber infinitesimal element subjected to curing.

The actual temperature of a point inside an item subjected to heating is, indeed, rather variable and such variability can be estimated only resorting to numerical methods. In general, each point **P** of the item has its own temperature profile $T = T(\mathbf{P}, t)$. At a fixed time during the curing process, each point has also its own torque value, which can be calculated from the database collected previously. For each value of the torque reached, a corresponding value of the output parameter can be identically evaluated. In this way, torque-exposition time and output property-exposition time (or alternatively output property-temperature) profiles can be numerically estimated. Nonetheless, Figure 7 gives a precise (although approximate) idea of the complex

TABLE II
Rheometer Output Data Obtained for Dutral 4334 Blend at Two Different Imposed Temperatures

Temperature (T)	160°C	200°C
Minimum torque	15 dNm	7 dNm
Scorch torque	20 dNm	12 dNm
t_2-scorch time	150 sec	50 sec
t_{90}-torque	58 dNm	52 dNm
t_{90}– 90% vulcanization time	700 sec	200 sec
de vulcanization torque	60 dNm	54 dNm
de vulcanization time	2800 sec	900 sec

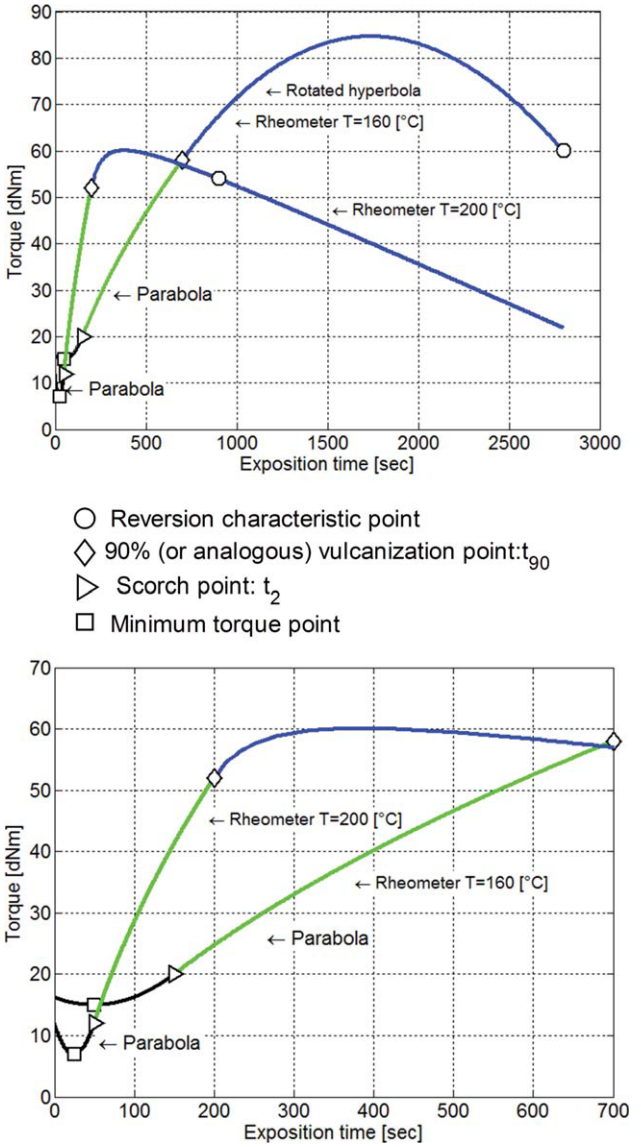

Figure 6 Rheometer numerical curves at increasing controlled temperatures (Dutral TER 4334). [Color figure can be viewed in the online issue, which is available at wileyonlinelibrary.com.]

behavior of rubber during vulcanization, addressing that a strong variability of output mechanical properties is obtained changing curing time and vulcanization temperature.

3D RUBBER THICK ELEMENTS VULCANIZATION THROUGH SULFUR

Sulfur vulcanization kinetics is not analytically known and no mathematical formulations commonly accepted are available in the literature, as it occurs for instance with peroxidic curing or silicon vulcanization.[32–36] Several efforts have been made in the past to propose simple numerical approaches able to describe the state of cure of rubber vulcanized with

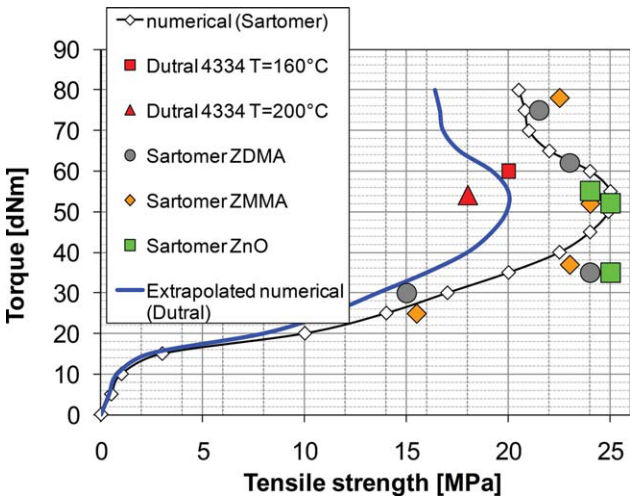

Figure 7 Numerical relation between tensile strength and torque used in the simulations regarding the industrial process optimization (Dutral TER 4334 and Sartomer Natsyn 2200 rubber compounds). [Color figure can be viewed in the online issue, which is available at wileyonlinelibrary.com.]

sulfur. Among the others, some pioneering contributions go back to 1960s (see Smith and coworkers).[37,38] Afterward, interesting and easy to use successful models have been presented by Kamal and Sourour,[39] Ding and Leonov,[8] Ding et al.[9] and Duchacek and Duskova.[40]

Essentially, all these models are numerical approaches based on a sort of experimental data fitting (as that used in this article), which are enforced to resemble to peroxidic laws. As the aim of this article is to give only a macroscopic description of the vulcanization process, a correlation between cure curve and (largely unknown) sulfur vulcanization kinetics is avoided, and a simple cure curve data fitting is proposed.

Considering the extreme complexity of the problem, nowadays, empirical approaches and rule of thumbs are therefore preferred by practitioners. However, manufactures are unable to guarantee a defined level of vulcanization for thick items and such cured elements are almost always of poor quality, precluding their widespread in engineering applications. During the vulcanization process, indeed, an inhomogeneous distribution of temperatures between internal (cool) zone and (hot) skin occurs.

TABLE III
Output Mechanical Properties Obtained for Dutral 4334 Blend at Two Different Imposed Temperatures

Temperature T [°C]	160	200
σ_t-tensile strength [MPa]	20	18
$\varepsilon_{\%}$- elongation % at failure	230	325

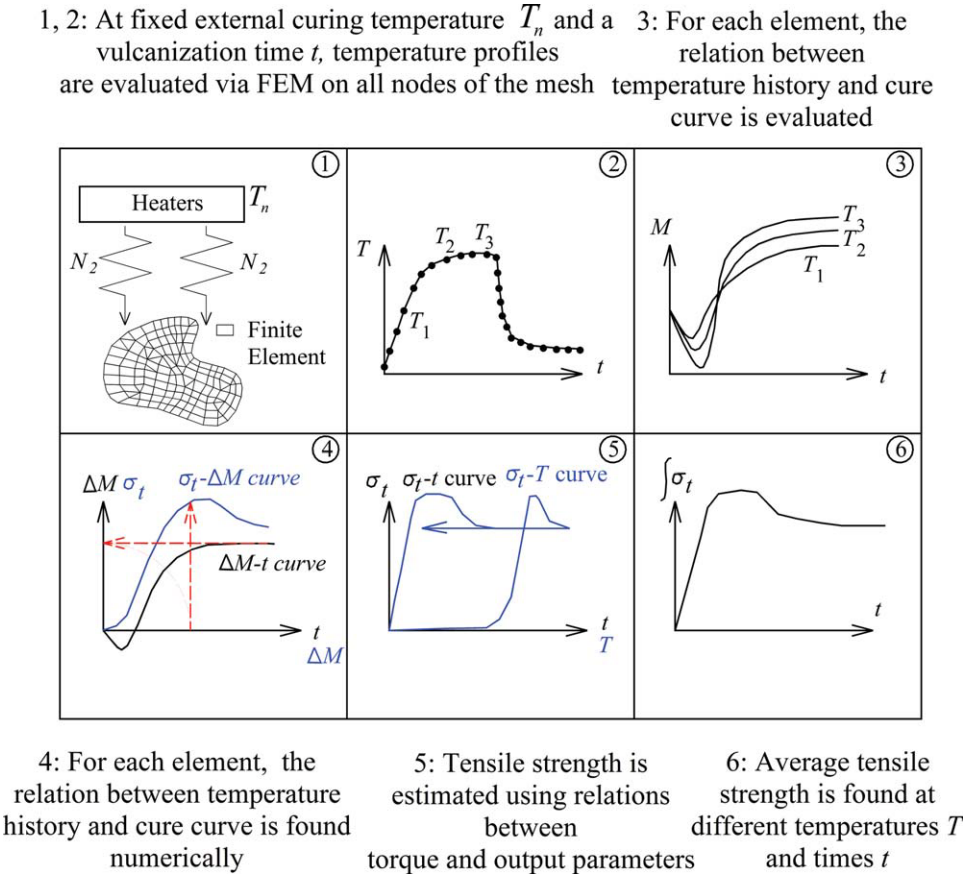

Figure 8 Schematic representation of the optimization process phases. [Color figure can be viewed in the online issue, which is available at wileyonlinelibrary.com.]

With the aim of optimizing a production line, many parameters have to be chosen carefully. In particular, the variables, exposition time and temperature of the heating phase, play a crucial role.

Basics of the numerical model adopted

The software presented in this article is an assemblage of the following elemental blocks, which are also graphically summarized in Figure 8.

1. At fixed values of the input parameters T_n and t_c, for each node of the item (already discretized by means of Finite Elements) temperature profiles are numerically evaluated solving Fourier's heat transmission law in 2D/3D dimensions.[17–36,41] Here, it is worth underlining that, in the most general case, Fourier's equation is partial and differential, therefore a finite element (FEM)[42] discretization is needed. For each node of the item and for each value of exposition time and curing temperature inspected numerically, local final mechanical properties are evaluated. Uniaxial tensile strength is considered as objective function. As we are interested in evaluating the overall properties of the vulcanized rubber, an averaged objective function is adopted (i.e. the mean tensile strength is maximized). To maximize this quantity, the following sub-blocks are repeated for each node:
   a. At increasing times, the temperature of each node varies (increasing until the end of the vulcanization range and then suddenly decreasing in the cooling phase). Thus, during the simulation, each point is characterized by a temperature corresponding to a time value.
   b. For each temperature value collected in the previous sub-block, the corresponding cure curve (stored in the database built in step 1) is uploaded. Here, it is worth noting that each node of the item to vulcanize undergoes continuously different temperatures, thus passing from a cure curve to a contiguous one increasing the time (more precisely to a contiguous curve associated to a higher temperature in the heating phase).
   c. For each node of the item, the torque-time diagram is evaluated making use of all the cure curves uploaded in the previous substep.

d. Tensile strength is finally evaluated (tensile strength-time and tensile strength-temperature may also be plotted) for each node as a function of the torque (obtained in the previous substep) reached by the point at successive time steps. This operation is possible only having at disposal a relation between final torque and tensile strength (usually experimental data are available).

2. The procedure summarized in point 1) should be repeated changing input parameters (i.e. total curing time and vulcanization agent temperature). The most direct way to evaluate the best choice for the couple (t_cT_n) is probably to subdivide the input domain in a regular grid of points. Refining the grid allows a more precise evaluation of the optimal input parameters, but requires a huge computational effort. For this reason, an alternating tangent (AT) procedure is here adopted. Such method, already presented in[43] requires to proceed through sections at T_n or t fixed, in bounding the remaining undetermined variable at the first iteration, in evaluating tensile strength first derivatives at the extremes and at the middle point of the interval inspected and in bisecting iteratively the interval on the base of first derivative sign.

The heat transmission problem modified

A modified heat transmission problem has to be solved to evaluate item temperature profiles, accounting for the chemical reactions occurring during vulcanization. We schematically subdivide the curing process into two phases, the heating and the cooling one. In the first phase, elastomers are exposed to high temperatures to activate cross-linking and thus vulcanization, whereas in the second rubber is kept to ambient temperature through air and/or water.

In the most general case of 3D items, temperature profiles for each point of the element are obtained solving numerically Fourier's heat equation law[41]

$$\rho_p c_p^p \left(\frac{\partial T}{\partial t}\right) - \lambda_p \nabla^2 T - r_p \Delta H_r = 0 \qquad (3)$$

where ρ_p, c_p^p, and λ_p are EPDM density, specific heat capacity, and heat conductivity respectively; ΔH_r is rubber specific heat (enthalpy) of reaction and is expressed in kJ mol^{-1}; r_p is the rate of cross-linking and is expressed in mol/(m^{3}sec).

Boundary and initial conditions

When heat transmission at the external boundary is for convection + radiation (extrusion process), the following boundary conditions must be applied:

$$\lambda_p \frac{\partial T(\mathbf{P},t)}{\partial \mathbf{n}(\mathbf{P})} + h(T(\mathbf{P},t) - T_n) + q_{\text{rad}} = 0 \qquad (4)$$

where, h is the heat transfer coefficient between EPDM and vulcanizing agent at fixed temperature T; T_n is vulcanizing agent (e.g. nitrogen) temperature; $\mathbf{P}$ is a point on the object surface and $\mathbf{n}$ is the outward versor on $\mathbf{P}$; q_{rad} is the heat flux transferred by radiation. Radiation contribution for the vulcanization of complex 2D geometries may not be determined precisely. At a first glance, the simplified following formula is applied:

$$q_{\text{rad}} = \sigma\left(T_n^4 - T\left(R_p,t\right)^4\right) \Big/ \left[1/\varepsilon_p + \frac{A_p}{A_n}(1/\varepsilon_n - 1)\right] \qquad (5)$$

where $\sigma = 5.67 \cdot 10^{-8} \frac{W}{m^2 K^4}$ is the Stefan-Boltzmann constant, $\varepsilon_{p,n}$ are emissivity coefficients, $A_{p,n}$ are the areas of heat exchange (p: rubber item, n: curing agent).

The same considerations can be repeated for the cooling phase, substituting nitrogen temperature with the actual cooling agent temperature and assuming that heat exchange for radiation is negligible, that is,

$$\lambda_p \frac{\partial T(\mathbf{P},t)}{\partial \mathbf{n}(\mathbf{P})} + h_w(T(\mathbf{P},t) - T_w) = 0 \qquad (6)$$

where h_w is the water (air) heat transfer coefficient, T_w is the water (air) cooling temperature, and all the other symbols have been already introduced.

Initial conditions on temperatures at each point at the beginning of the curing process are identically equal to the ambient temperature (hereafter fixed equal to 25°C for the sake of simplicity), whereas initial conditions at the beginning of the cooling phase are obtained from the temperature profiles evaluated at the last step of the cooling zone, that is, at $T(\mathbf{P},t_c)$, where t_c is the total curing time and $\mathbf{P}$ is a generic point belonging to Ω.

Ad hoc finite element software

A numerical approach for solving partial differential equations system (3)–(6) is needed for complicated geometries and boundary conditions (as is the case here treated). Therefore, in what follows, a Finite Element (FEM)[32,33,42] discretization of the domain is utilized to obtain a reliable approximation of temperatures at each element point and at successive time steps. The procedure has been completely implemented in Matlab[44] language. In this

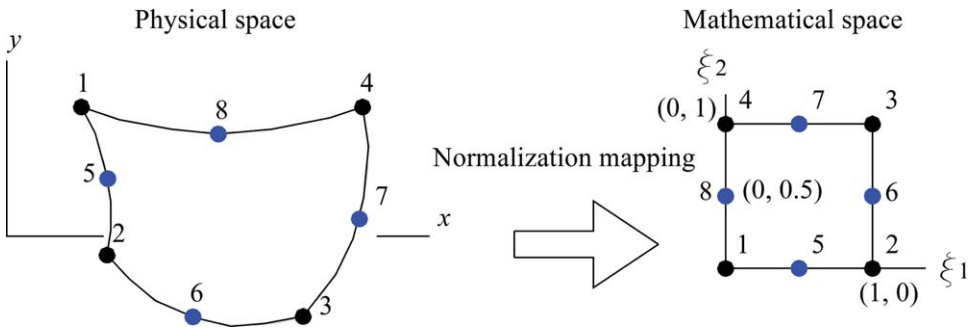

Figure 9 Eight-noded plane elements used for the 2D thermal transient analyzes (left: physical space, right: mathematical space). [Color figure can be viewed in the online issue, which is available at wileyonlinelibrary.com.]

way, resultant FE temperature profiles at each time step are directly collected from the numerical analysis and utilized for the evaluation of output rubber mechanical properties by means of an integrated tool.

When dealing with a generic extruded 2D rubber item, 8-noded plane elements have been used, see Figure 9. Temperature field interpolation is assumed polynomial inside each element, that is,

$$T(\mathbf{P}) = \mathbf{N}^e\mathbf{T}^e \tag{7}$$

where $\mathbf{T}^e = [T^1T^2 \ldots T^8]^T$ is the vector of nodal temperatures, $\mathbf{N}^e = [N^1N^2 \ldots N^8]$ is the vector of so-called shape functions N^i ($i = 1, \ldots 8$), $\mathbf{P}$ is a point of coordinates x_P, y_P, and z_P inside the element.

Indicating with $\mathbf{X}_i = (x_i, y_i, z_i)$ elements nodes coordinates, N^i are expressed by the following relation:

$$\mathbf{X} = \sum_{i=1}^{8} N_i(\xi_1, \xi_2, \xi_3)\mathbf{X}_i$$

$$N^i = \begin{cases} \frac{1}{4}\left(1+\xi_1^i\xi_1\right)\left(1+\xi_2^i\xi_2\right)\left(\xi_1^i\xi_1+\xi_2^i\xi_2-1\right) & i=1,2,3,4 \\ \frac{1}{2}\left(1-(\xi_1)^2\right)\left(1+\xi_2^i\xi_2\right) & i=5,6 \\ \frac{1}{2}\left(1-(\xi_2)^2\right)\left(1+\xi_1^i\xi_1\right) & i=7,8 \end{cases} \tag{8}$$

where $\xi_i \in [0\ 1]$ is a normalized coordinate and vertices are obtained alternatively imposing $\xi_j = 1$ and $\xi_i = 0$ and vice versa.

In the numerical simulations reported, the following parameters have been used: EPM/EPDM density $\rho_p = 922$ Kg m^{-3}, rubber specific heat capacity $c_p^p = 2700$ J/(kg °C), $\lambda_p = 0.335$ W/(m°C), $\Delta H_r = 180$ kJ mol^{-1}, water heat transfer coefficient $h_w = 1490.70$ W/(m^2°C), curing agent heat transfer coefficient $h = 900$ W/(m^2°C) [for air heat transfer coefficient we assume $h = 5$ W/(m^2°C)], $\varepsilon_p = 0.60$, $\varepsilon_c = 0.70$, water cooling temperature $T_w = 25$°C.

The geometry of the 2D rubber item analyzed in this article is sketched in Figure 10. In Figure 11, color patches representing temperature profiles

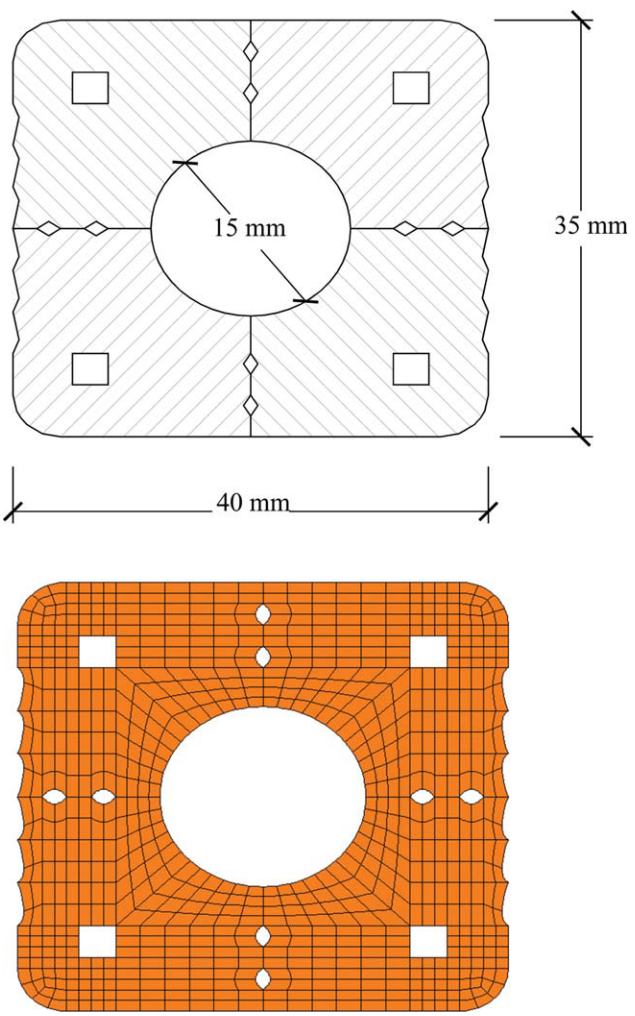

Figure 10 Geometry and FEM discretization by means of eight-noded elements (2552 nodes, 780 plates). [Color figure can be viewed in the online issue, which is available at wileyonlinelibrary.com.]

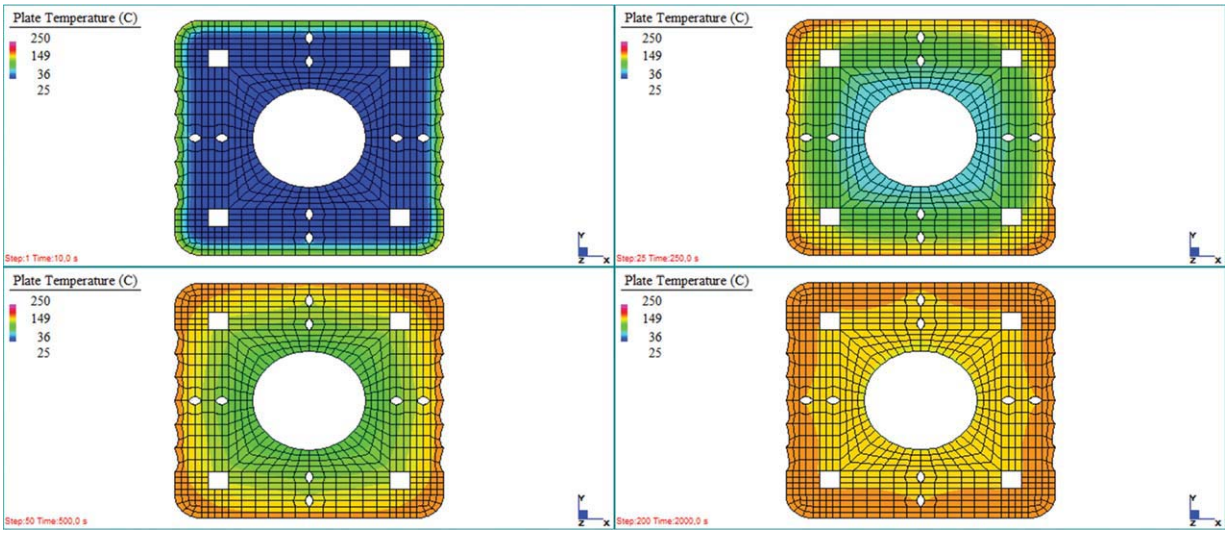

Figure 11 Snapshots from the FEM program representing temperature profiles at increasing exposition times (T_n = 180°C). [Color figure can be viewed in the online issue, which is available at wileyonlinelibrary.com.]

obtained during a FEM simulation at increasing instants are represented (T_n = 180°C is assumed). As it is possible to notice, internal points heating is sensibly slower with respect to the skin. This influences significantly the final quality of the vulcanized rubber.

To have an insight into the predictive capabilities of the numerical approach proposed point by point, the thermal behavior during vulcanization of two points belonging respectively to the internal region (Point A) and to the external skin (Point B) is represented in Figures from 12 to 15. The temperature profile of Point A, represented in Figure 13 (bottom-right), shows a moderate initial temperature increase, meaning that Point A passes from rheometric curves at low temperatures to rheometric curves at high temperatures slowly. Such curves are numerically interpolated, as already pointed out, from experimental data available for the rubber compound inspected, see Figure 6.

When the maximum temperature is reached, Point A follows the rheometric curve relative to such temperature, stabilizing its behavior at increasing times on that rheometer curve. In other words, point A follows almost completely the rheometer curve at 180°C, even in the reversion branch. The relationship used to evaluate the final tensile strength of the point is depicted in Figure 7, which is a reasonable hypothesis of the compound behavior extrapolated from different data collected from Dutral compounds.[21] As the tensile strength peak is reached at ~ 54 dNm of torque and considering that the rheometer curve exhibits at 180° a reversion around at 72 dNm, it is expected that reversion is clearly deducible on the diagram curing time-tensile strength sensibly after the peak strength is reached.

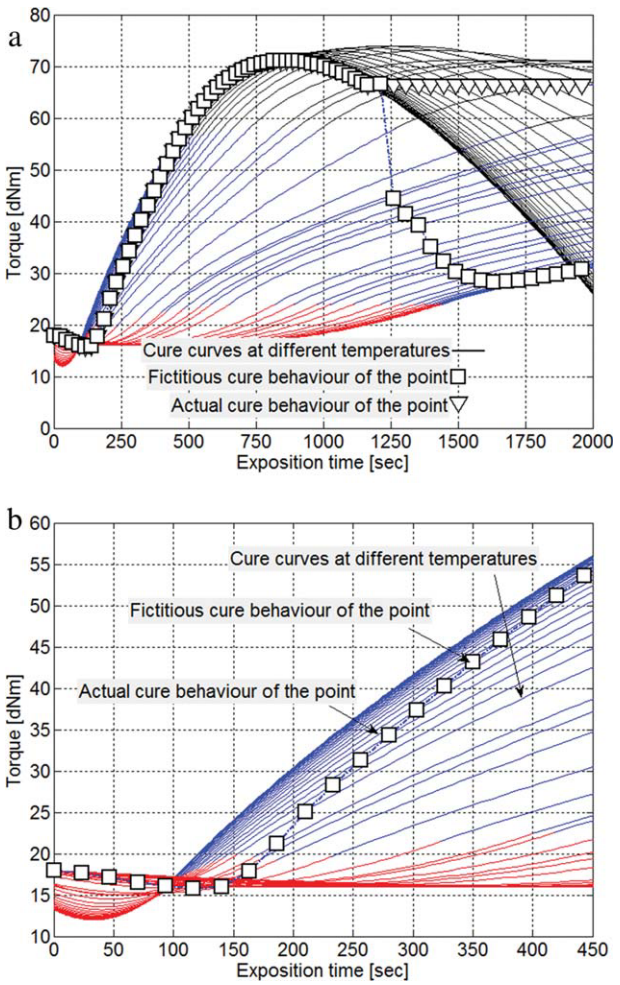

Figure 12 Point A behavior during vulcanization, passage from low temperature to high temperature cure curves. (a) Behavior during all the vulcanization process. (b) Detail in the first phase of the vulcanization. [Color figure can be viewed in the online issue, which is available at wileyonlinelibrary.com.]

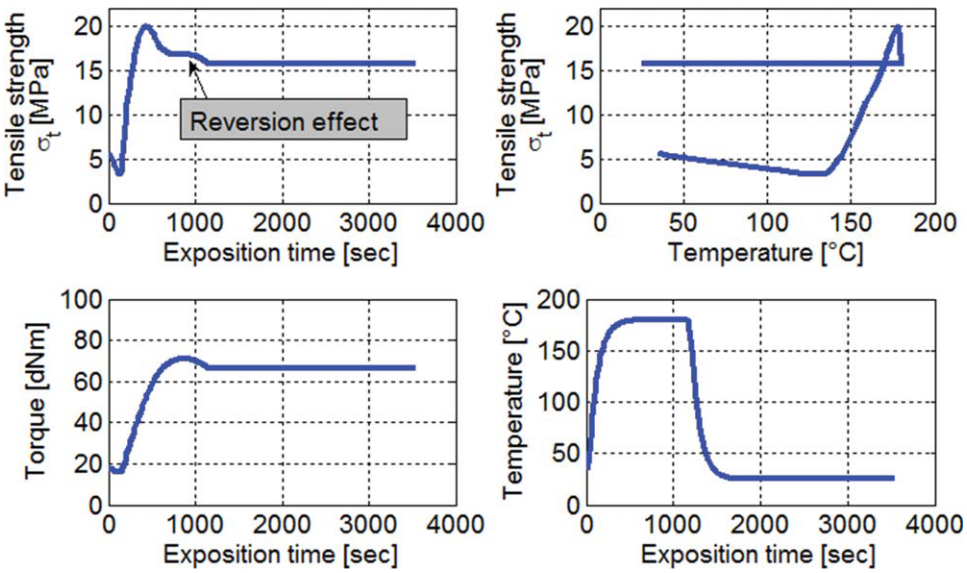

Figure 13 Point A mechanical properties evolution during vulcanization. Top-left: exposition time-tensile strength diagram. Top-right: temperature-tensile strength diagram. Bottom-left: exposition time-torque diagram. Bottom-right: temperature profile. [Color figure can be viewed in the online issue, which is available at wileyonlinelibrary.com.]

When the curing finishes, temperature decreases quickly. Here, two paths should be followed numerically for Point A, represented in Figure 12 with squares and triangles. The numerical behavior represented by squares is not real, because it would be referred to a material without any memory of the vulcanization. Therefore, it relies on a compound that ideally jumps from a rheometer curve at high temperature to the successive at low temperature (reversible process). On the contrary, the real behavior of the material under consideration is represented by the triangles, indicating that the level of vulcanization reached at the end of the curing process cannot be inverted reducing temperature, but can only be stopped.

Once that the curing time-torque diagram of the rheometric curve is known numerically (bottom-left diagram) for the point under consideration, tensile strength reached increasing exposition times can be easily determined through the relation sketched in Figure 7. For point A, the exact vulcanization history in terms of curing time-σ_t and temperature-σ_t diagrams is represented in Figure 13 (top sub-figures).

The instant at which reversion starts is particularly clear, with a sensible decrease of the final tensile strength of the point. As already pointed out, reversion occurs after that the peak strength is reached, because of the numerical torque-tensile strength relationship assumed in input (Fig. 7). Therefore, it can be argued that, in this case, the reversion problem occurs always for curing times successive to those near the optimal vulcanization regime.

The same considerations can be repeated for any point of the item, thus giving the possibility to

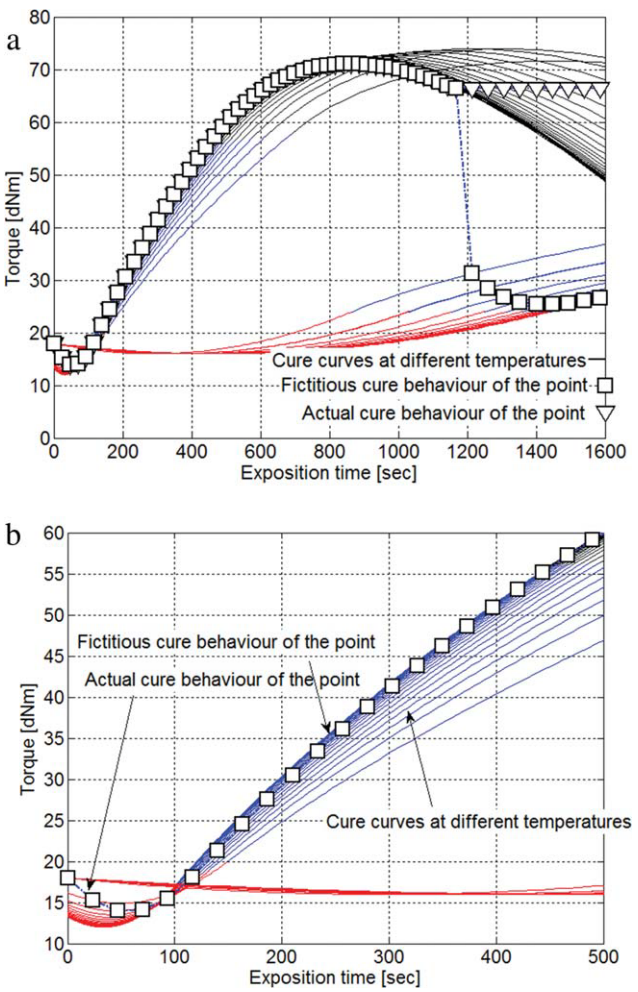

Figure 14 Point B behavior during vulcanization. (a) Behavior during all the vulcanization process. (b) Detail in the first phase of vulcanization. [Color figure can be viewed in the online issue, which is available at wileyonlinelibrary.com.]

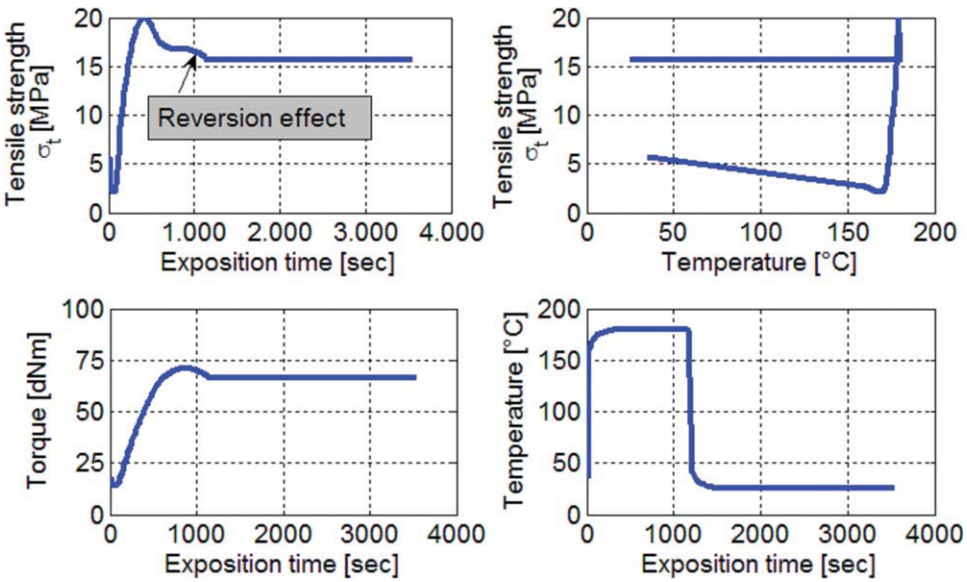

Figure 15 Point B mechanical properties evolution during vulcanization. Top-left: exposition time-tensile strength diagram. Top-right: temperature-tensile strength diagram. Bottom-left: exposition time-torque diagram. Bottom-right: temperature profile. [Color figure can be viewed in the online issue, which is available at wileyonlinelibrary.com.]

evaluate the average final tensile strength. For instance, in Figures 14 and 15, the behavior during curing of a point near the external surface of the item (hereafter called Point B) is represented. From Figure 14, it is rather evident that Point B reaches maximum vulcanization temperature more quickly with respect to Point A, because the cure curves followed by the point are very near one each other. Also in this case, the reversion range is rather clear and, as expected, it occurs after that the peak strength has been reached.

From a detailed analysis of point A and point B behavior, it can be argued that a generalized over-vulcanization of the item has been obtained in this case, because the maximum tensile strength is reached before the end of the curing process in both cases, with a consequent decrease of final mechanical properties at the end of the simulations.

To inspect a case where reversion occurs almost contemporarily to the reaching of the peak value of tensile strength, the numerical relationship between torque and tensile strength depicted in Figure 16 is assumed as input property of the compound (second mechanical hypothesis). The same simulations presented previously for Point A and Point B assuming the diagram of Figure 7 are repeated here with the new assumption.

Results in terms of temperature profiles (the same of the previous simulations), torque-curing time (bottom-left), tensile strength-curing time (upper-left), and tensile strength-temperature (upper-left) are summarized in Figures 17 and 18 respectively for Point A and Point B. In this case, reversion occurs immediately after the maximum value of tensile strength has been reached, meaning the curing time has to be reduced to avoid an unpleasant reduction of the final mechanical properties of the item, because of over-vulcanization and reversion of sulfur reactions at the end of the vulcanization process. The technical usefulness of Figures 17 and 18 results appears to the authors rather clear, as manufacturers could calibrate (with a few numerical attempts) both curing time and vulcanization temperature of the production phase to avoid reversion.

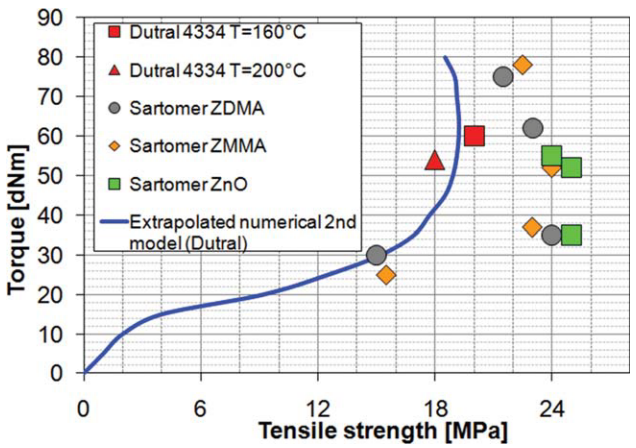

Figure 16 Second numerical relation (hypothesis) between tensile strength and torque used to demonstrate the effect of reversion (Dutral TER 4334 rubber compound). [Color figure can be viewed in the online issue, which is available at wileyonlinelibrary.com.]

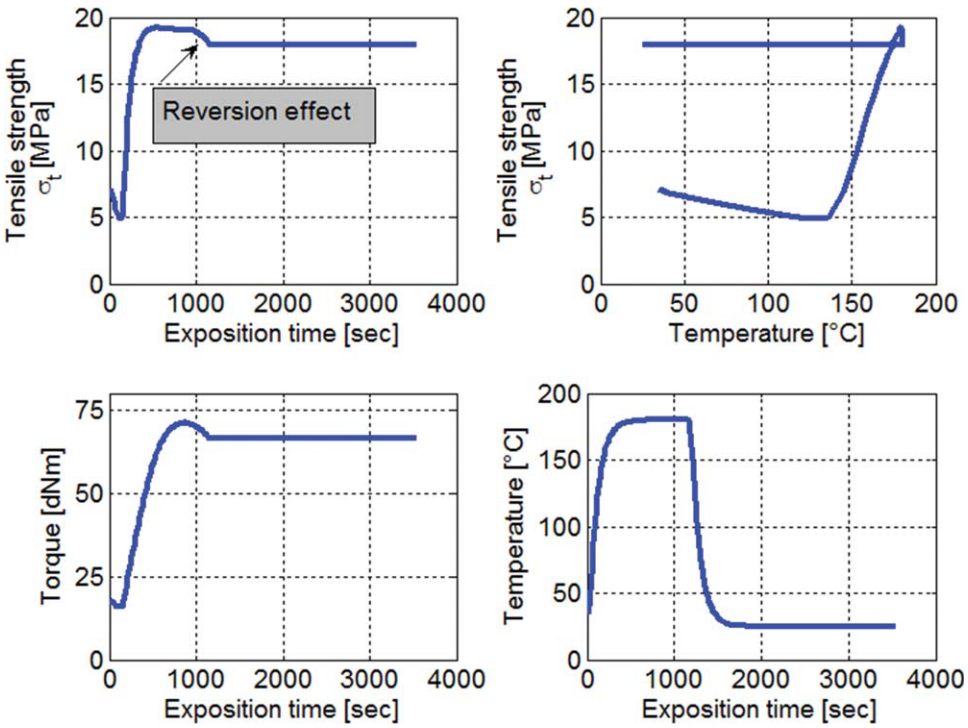

Figure 17 Point A mechanical properties evolution during vulcanization (second numerical hypothesis). Top-left: exposition time-tensile strength diagram. Top-right: temperature-tensile strength diagram. Bottom-left: exposition time-torque diagram. Bottom-right: temperature profile. [Color figure can be viewed in the online issue, which is available at wileyonlinelibrary.com.]

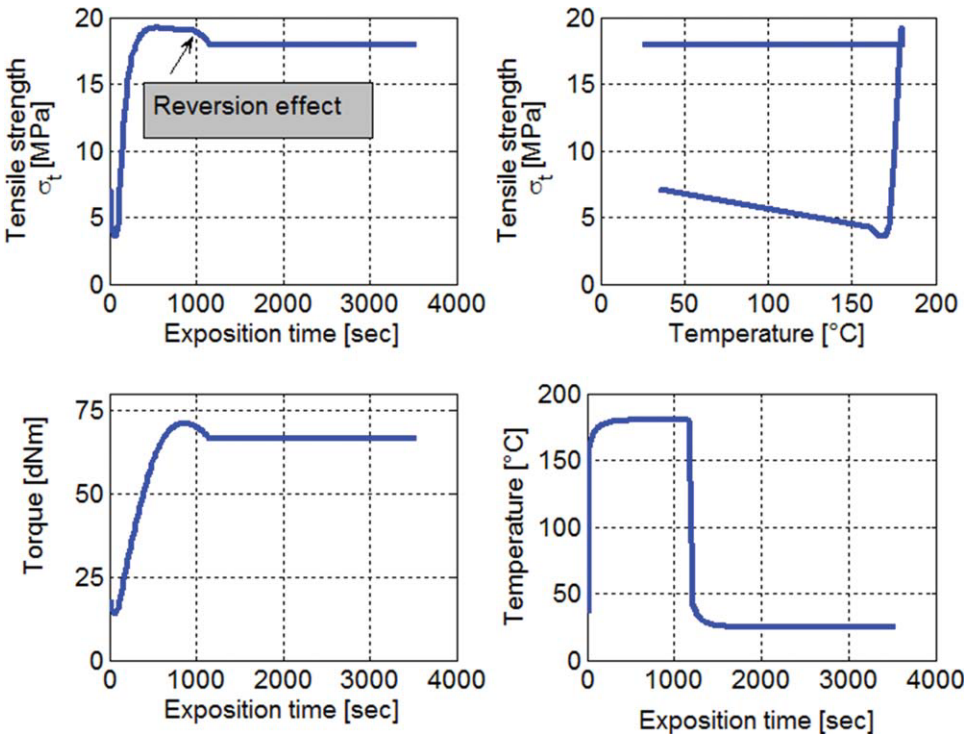

Figure 18 Point B mechanical properties evolution during vulcanization (second numerical hypothesis). Top-left: exposition time-tensile strength diagram. Top-right: temperature-tensile strength diagram. Bottom-left: exposition time-torque diagram. Bottom-right: temperature profile. [Color figure can be viewed in the online issue, which is available at wileyonlinelibrary.com.]

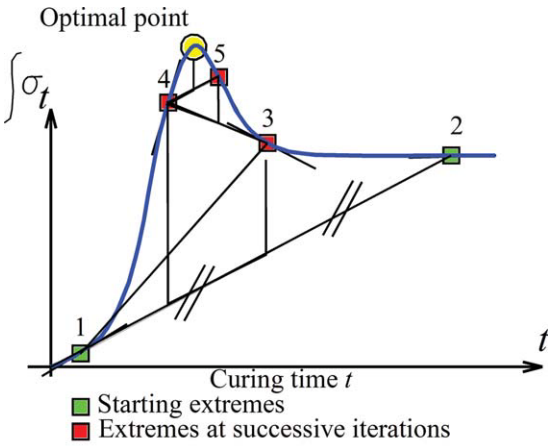

Step 0: evaluate first derivative at points 1 and 2
Step 1: evaluate first derivative at point 3 (mean value between abscissae 1 and 2)
Step 3: select the new extreme of the interval on the bases of the sign of 3 first derivative (negative 1-3 positive 3-2)
Step 4: repeat Step 1 substituting original points with the new extremes

Figure 19 Alternating tangent approach (AT) basic scheme. [Color figure can be viewed in the online issue, which is available at wileyonlinelibrary.com.]

IMPROVING THE NUMERICAL EFFICIENCY OF OPTIMIZATION: ALTERNATING TANGENT APPROACH

The approach used in this article was originally developed by Milani and Milani,[43] and the reader is referred there for a detailed description of the method used. It is a bisectional procedure based on the numerical evaluation of tensile strength first derivatives with respect to exposition time on several sections at fixed curing temperatures T_n and on the iterated bisection of a determined exposition time search interval, see also Figure 19.

At a fixed T_n temperature, tensile strength is evaluated on the two extremes of the interval (points 1 and 2), usually placed at a very under-vulcanized and a very over-vulcanized exposition time.

It is worth noting that the procedure proposed converges also at fixed exposition times and varying nitrogen temperature T_n, therefore numerical simulations can be performed using two "perpendicular" different strategies.

First derivatives $d\sigma_t/dt$ of tensile strength with respect to exposition time are needed at the search interval extremes. Since $d\sigma_t/dt$ are not known analytically, a numerical procedure based on finite differences is adopted. They are evaluated considering tensile strength at a point 1′ with exposition time equal to 1 plus a small increment Δt and at a point 2′ with exposition time equal to 2 decremented of a small Δt. Tensile strength is then evaluated in 1′ and 2′, thus giving the possibility to evaluate first derivatives at 1 and 2 through finite differences. Δt is usually fixed in the range 1–3 sec to obtain reliable results. Middle point first derivative of the search interval is also needed, as depicted in Figure 19.

Once that first derivatives are at disposal on the search interval extremes and on the middle point, a bisection procedure is adopted, reducing the search interval to one-half. In particular, the new interval is respectively the right or the left one-half depending on the sign of first derivatives of the extremes with respect to the middle point one, that is,

$$\text{if } \left.\frac{d\sigma_t}{dt}\right|_1 \cdot \left.\frac{d\sigma_t}{dt}\right|_3 \geq 0 \rightarrow \text{select right semi} - \text{interval}$$
$$\text{if } \left.\frac{d\sigma_t}{dt}\right|_2 \cdot \left.\frac{d\sigma_t}{dt}\right|_3 \geq 0 \rightarrow \text{select left semi} - \text{interval} \quad (9)$$

The procedure is repeated iteratively on the new half-interval, bounding more and more strictly the actual optimal solution at the new iteration. The algorithm is stopped until a desired degree of accuracy is obtained (circle in Fig. 19).

NUMERICAL SIMULATIONS

A set of numerical simulations is reported in this section, to show the capabilities of the experimental-numerical procedure proposed in predicting the vulcanization of real items. Numerical results refer to the temperatures database collected from the FEM model of Figure 10. In particular, a number of thermal analyzes have been performed changing curing temperature T_n and exposition time $t = t_c$ and assuming the numerical relation between tensile strength and torque shown in Figure 16. We suppose that the item is constituted by Dutral TER 4334.

The approach proposed allows to estimate optimal input parameters functions $\hat{T} = \hat{T}(T_n, t_c) = 0 \mid \hat{T} \equiv \{P^i = (T_n^i, t_c^i)\text{optimal}\}$. In particular, optimal $\hat{T}$ curves (expressed as implicit functions in T_n and t_c) are numerically evaluated solving the following optimization problem through bisection, once that one of the input parameters T_n^i or t_c^i is a priori fixed (sectional approach):

$$\max \frac{1}{N_L}\sum_{k=1}^{N_L}\sigma_t^k(T_n^i, t_c^i)$$

$$\text{subject to}\begin{cases} T_n^i = \text{fixed} \\ t^{\min} < t_c^i < t^{\max} \end{cases} \tag{10}$$

$$\text{PDEs system}\begin{cases} \rho_p c_p^p\left(\frac{\partial T}{\partial t}\right) - \lambda_p \nabla^2 T - r_p \Delta H_r = 0 \\ \text{boundary and initial conditions} \end{cases}$$

where N_L is the number of nodes in which the item is discretized and $t^{\min}$ ($t^{\max}$) is a lower (upper) bound limitation for curing temperature.

Results provided by the alternating tangent approach proposed are compared with those obtained subdividing $T_n - t_c$ plane with a regular grid. In the latter case, for each point $P^{i,j} \equiv (T_n^i, t_c^j)$ of the grid a mixed algebraic-PDEs system has to be solved:

$$\sigma_t = \frac{1}{N_L}\sum_{k=1}^{N_L}\sigma_t^k(T_n^i, t_c^j)$$

$$\text{PDEs system}\begin{cases} \rho_p c_p^p\left(\frac{\partial T}{\partial t}\right) - \lambda_p \nabla^2 T - r_p \Delta H_r = 0 \\ \text{boundary and initial conditions} \end{cases} \tag{11}$$

Obviously a very large computational effort is required in solving problem (11), especially for very refined discretizations (as those needed in the present simulations) using the grid method (otherwise a global optimization algorithm where objective function is not analytically known has to be performed).

Results of the performed simulations are summarized in Figure 20, where the average final tensile strength at different temperatures and exposition times is depicted. The 3D surface results from an expensive subdivision of the domain into a regular grid of points. Each resultant tensile strength is obtained solving (11) through the Finite Element procedure previously described. Squares represent the optimal points obtained with the bisectional approach, whereas circles are the successive intervals extremes and diamonds the initial intervals. As can be deducted from the figures, the bisectional algorithm adopted allows to reduce drastically computational time needed.

In this case, simulations are performed fixing curing temperature and bisecting exposition time.

In Figure 21, results for two fixed curing temperatures (160° and 220°) and varying exposition time are reported. The continuous curve is an expensive section obtained with the grid method, with a grid of 10,000 curing times and fixed temperature. A very refined grid is needed because peaks may be very narrow. Squares, circles, and diamonds are bisectional iterated solutions.

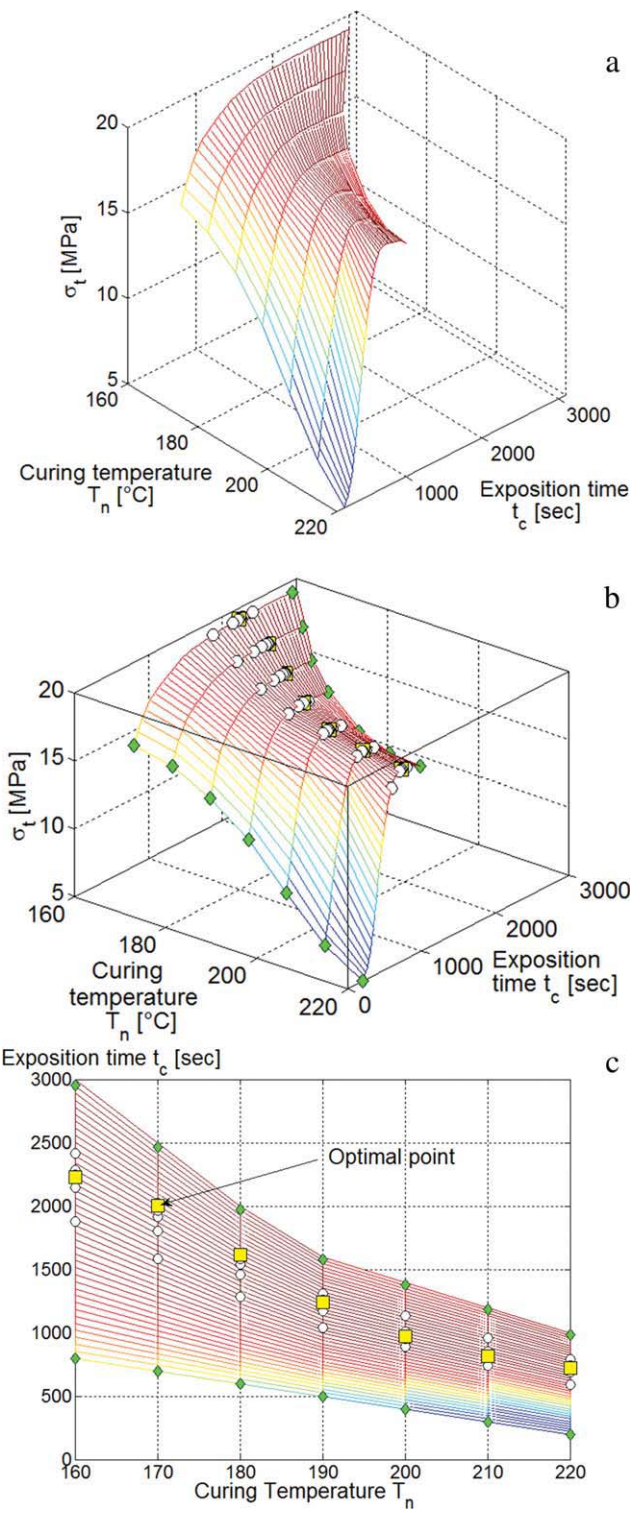

Figure 20 2D thick item. Optimal output tensile strength at different values of exposition time and nitrogen temperature. (a) 3D view (grid method only).(b) 3D view with sectional approach (squares, circles and diamonds represent AT approach results). Squares are final optimized points form AT approach, circles extremes of the successive intervals inspected, diamonds initial search intervals.(c) Aerial view of optimized results. [Color figure can be viewed in the online issue, which is available at wileyonlinelibrary.com.]

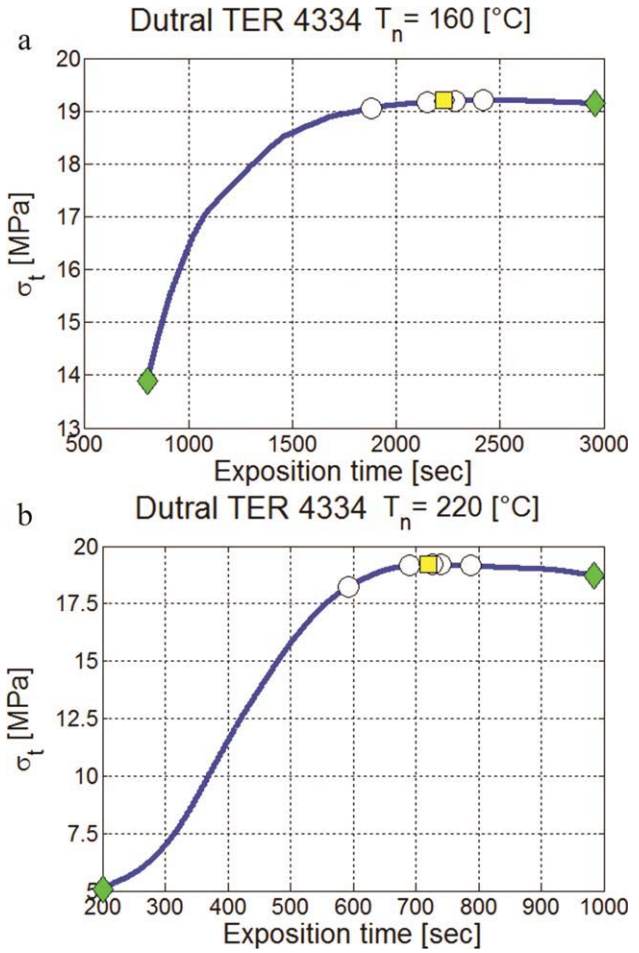

Figure 21 2D vulcanized item. Optimal output tensile strength at different values of exposition time and fixed value of curing temperature. (a) T_n = 160°C; (b) T_n = 220°C. The continuous lines represent results from the grid method, whereas squares, circles, and diamonds represent AT approach results. [Color figure can be viewed in the online issue, which is available at wileyonlinelibrary.com.]

As a matter of fact, because of the item thickness, considerable differences on optimal points are observed varying curing temperatures in a wide range. A comparison regarding optimal points obtained increasing curing temperature from 160° to 220° with a step equal to 10°C is depicted in Figure 22.

The technical usefulness of Figures 20 and 22 is worth noting. In particular, once that a compound with fixed cure curves at different temperatures is considered, producers can enter in the figures with a desired curing temperature (exposition time) and exit with the optimal exposition time (curing temperature) for the production line.

CONCLUSIONS

A numerical procedure for the determination of optimal input parameters -in presence of reversion- for 2D thick rubber items vulcanized with accelerated sulfur has been presented. Curing external temperature T_n and rubber exposition time t have been assumed as production parameters to optimize, whereas objective function was represented by rubber final mean tensile strength.

The procedure relies into two steps. In the first step, at a fixed rubber compound, rheometer cure curves at different temperatures have been collected and fitted with a composite, first derivative continuous, three function curve obtained by the assemblage of two parabolas and a rotated hyperbola. Rheometer test is probably the most suitable way to collect indirect information on the rubber reticulation kinetics at different temperatures. It has been avoided to follow kinetics appeal and it has been preferred a "crude" experimental data fitting. Several comparisons with existing literature have been reported to test the capabilities of the model proposed. In particular, it has been shown that, assuming a suitable angle of rotation of the hyperbola, the model gives good predictions of the reversion phenomenon in a very wide range.

Some real cure curves at different temperatures have been collected, fitted numerically and exported in a suitable database to use in the second step for the prediction of the optimal vulcanization of real thick elements industrially produced. A meaningful example of engineering interest, consisting of a thick 2D EPDM item with rectangular shape has been analyzed using non standard Finite Elements and thermal analyzes, to validate the model and to show the efficiency of the numerical procedure developed.

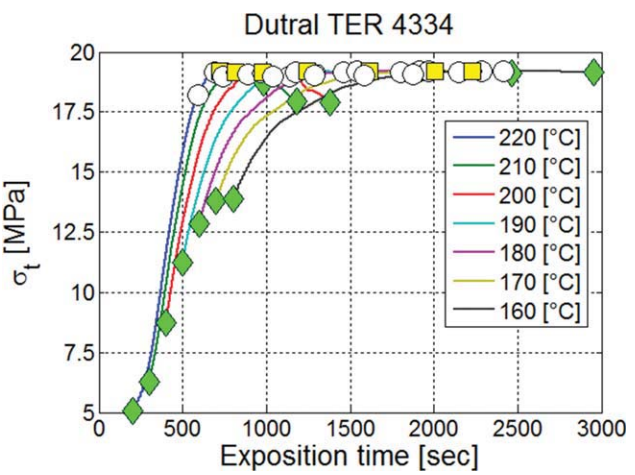

Figure 22 2D vulcanized item. Optimal output tensile strength at different values of exposition time and fixed value of curing temperature. Simulations from 160 to 220°C. The continuous lines represent results from the grid method, whereas squares, circles, and diamonds represent AT approach results. [Color figure can be viewed in the online issue, which is available at wileyonlinelibrary.com.]

Finally, it is stressed that the complex numerical procedure proposed is strictly theoretical and the prediction of the actual average mechanical properties of thick items remains, of course, an open issue. A work in progress by the authors is an experimental assessment of the numerical approach proposed on thick simple geometries, which will be available soon.

References

1. Coran, A. Y. Science and Technology of Rubber, Academic Press: New York, 1978; Chapter 7.
2. Rakmatullina, A. P.; Akhmed'yanova, R. A.; Liakumovich, A. G.; Portnoi, Ts. B.; Mokhnatkina, E. G.; Il'yasov, R. S. Int Polym Sci Technol 2004, 31, 29.
3. Yamashita, S.; Kaneko, T. Handbook of Crosslinking Agents, Taiseisha: Tokio, 1981.
4. Yamashita, S.; Kaneko, T. Handbook of Crosslinking Aquipment, Taiseisha: Tokio, 1983.
5. Goodyear, C. U.S. Pat. 3,633 (1844).
6. Billmeier, F. W. Textbook of Polymer Science; 3rd ed.; John Wiley and Sons: New York, 1984.
7. Krejsa, M. L.; Koenig, J. L. Rubber Chem Technol 1993, 66, 376.
8. Ding, R.; Leonov, I. J Appl Polym Sci 1996, 61, 455.
9. Ding, R.; Leonov, I.; Coran Ay, A. Y. Rubber Chem Technol 1996, 69, 81.
10. Chen, C. H.; Koenigs, J. L.; Collins, E. A. Rubber Chem Technol 1981, 54, 734.
11. Loo, C. T. Polymer 1974, 15, 729.
12. Morrison, N. J.; Porter, M. Rubber Chem Technol 1984, 57, 63.
13. ASTM D 2084-81. Standard test methods for vulcanized rubber and thermoplastic elastomers-tension. Annual Book of ASTM Standards 1986.
14. Natta, G.; Crespi, G.; Mazzanti, G. Ethylene-propylene copolymers containing unsaturations. 4th Rubber Technology Conference; London, 1962
15. Natta, G.; Crespi, G.; Mazzanti, G. L'industria della gomma [the rubber industry] 1963, 1.
16. Morton, M., Ed. Rubber Technology, 2nd ed.; Van Nostrand Reinhold: New York, 1981.
17. Milani, G.; Milani, F. J Math Chem 2010, 47, 229.
18. Milani, G.; Milani, F. J Appl Polym Sci 2009, 111, 482.
19. Balasubramanian, M. J Polym Res 2009, 16, 133.
20. De Falco A. A.; Marzocca, A. J.; Corcuera, M. A.; Eceiza, A.; Mondragon, I.; Rubiolo, G. H.; Goyanes S, S. J Appl Polym Sci 2009, 113, 2851.
21. Henning, S. K. In Proceedings of the Spring 167th Technical Meeting of the Rubber Division; American Chemical Society: San Antonio, TX, May 16–18, 2005.
22. Arrillaga, A.; Zaldua, A. M.; Atxurra, R. M.; Farid, A. S. Eur Polym J 2007, 43, 4783.
23. Dick, J. S.; Pawlowski, H. Polym Test 1995, 14, 45.
24. Poh, B. T.; Wong, K. W. J Appl Polym Sci 1998, 69, 1301.
25. Poh, B. T.; Ng, C. C. Eur Polym J 1998, 34, 975.
26. Poh, B. T.; Chen, M. F.; Ding, B. S. J Appl Polym Sci 1996, 60, 1569.
27. Poh, B. T.; Te, C. S. J Appl Polym Sci 1999, 74, 2940.
28. Poh, B. T.; Tan, E. K. J Appl Polym Sci 2001, 82, 1352.
29. Poh, B. T.; Ismail, H.; Tan, K. S. Polym Test 2002, 21, 801.
30. Bateman, L., Ed. The Chemistry and Physics of Rubber-like Substances, MacLaren: London, 1963.
31. ASTM D412-83, D624–86, D4482–85. Standard test methods for vulcanized rubber and thermoplastic elastomers-tension. Annual Book of ASTM Standards 1986.
32. Jia, Y.; Sun, S.; Xue, S.; Liu, L.; Zhao, G. Polymer 2002, 44, 319.
33. Jia, Y.; Sun, S.; Xue, S.; Liu, L.; Zhao, G. Polymer 2002, 43, 7515.
34. Wang, X.; Jia, Y.; Feng, L.; An, L. Macromol Theory Simul 2009, 18, 336.
35. Kosar, V.; Gomzi, Z. Thermochim Acta 2007, 457, 70.
36. Kosar, V.; Gomzi, Z.; Sintic, K. Chem Eng Process 2007, 46, 83.
37. Smith, D. A.; Welding, G. N. Rubber Chem Technol 1963, 36, 835.
38. Redding, R. B.; Smith, D. A. J IRI 1970, 4, 198.
39. Kamal, M. R.; Sourour, S. Polym Eng Sci 1973, 13, 59.
40. Duchacek, V.; Duskova, M. J Polym Eng 2001, 21, 341.
41. Evans, G.; Blackledge, J.; Yardley, P. Numerical methods for partial differential equations, 2nd ed.; Springer-Verlag: Berlin, 2001.
42. Zienkiewicz, O. C.; Taylor, R. L. The Finite Element Method, McGraw-Hill: London, 1989; Vol. I.
43. Milani, G.; Milani, F. Macromol Theory Simul 2009, 18, 336.
44. The Mathworks, Matlab 7.4 User's Guide, http://www.mathworks.com/products/matlab/, Natick, MA (2007).